

**NASA TECHNICAL NOTE**



**NASA TN D-2334**

*c. 1*

LOAN COPY: RE  
AFWL (WLI)  
KIRTLAND AFB,

DL54997



TECH LIBRARY KAFB, NM

**NASA TN D-2334**

**EFFECTS OF DISTRIBUTED ROUGHNESS HEIGHT  
ON AERODYNAMIC CHARACTERISTICS  
AND BOUNDARY-LAYER TRANSITION  
OF A WING-BODY-TAIL CONFIGURATION  
AT A MACH NUMBER OF 1.61**

*by Roy V. Harris, Jr.*

*Langley Research Center*

*Langley Station, Hampton, Va.*



EFFECTS OF DISTRIBUTED ROUGHNESS HEIGHT ON  
AERODYNAMIC CHARACTERISTICS AND BOUNDARY-LAYER TRANSITION  
OF A WING-BODY-TAIL CONFIGURATION  
AT A MACH NUMBER OF 1.61

By Roy V. Harris, Jr.

Langley Research Center  
Langley Station, Hampton, Va.

NATIONAL AERONAUTICS AND SPACE ADMINISTRATION

For sale by the Office of Technical Services, Department of Commerce,  
Washington, D.C. 20230 -- Price \$0.50

EFFECTS OF DISTRIBUTED ROUGHNESS HEIGHT ON  
AERODYNAMIC CHARACTERISTICS AND BOUNDARY-LAYER TRANSITION  
OF A WING-BODY-TAIL CONFIGURATION  
AT A MACH NUMBER OF 1.61

By Roy V. Harris, Jr.  
Langley Research Center

SUMMARY

An investigation has been conducted in the Langley 4- by 4-foot supersonic pressure tunnel to determine the effects of three-dimensional roughness trips on the boundary-layer transition and the longitudinal aerodynamic characteristics of a wing-body-tail configuration at a Mach number of 1.61. The tests were made throughout a range of free-stream Reynolds numbers per foot from about 0.6 million to 8.0 million with the model angle of attack adjusted to produce zero lift. Tests were made without boundary-layer trips and with trips of different roughness heights. At three test Reynolds numbers, data were recorded throughout an angle-of-attack range from about  $-1^{\circ}$  to  $12^{\circ}$  with several roughness sizes and without the trip.

As would be expected, the data indicate that the larger roughness particles produce a fully turbulent boundary layer at a lower free-stream Reynolds number than the smaller roughness particles. At the highest Reynolds numbers per foot (greater than about  $6.0 \times 10^6$ ), the drag levels appear to increase above the theoretical turbulent level. This additional drag may be due to the roughness particles since at these Reynolds numbers the roughness-particle height is larger than the boundary-layer thickness. Within the range of Reynolds numbers for which the variations in zero-lift drag coefficient indicate fully turbulent flow in the model boundary layer, the drag increments due to the various sizes of roughness particles are small and within the accuracy of the drag data.

When the boundary layer was not fully turbulent at zero lift, small increases in the lift coefficient produced drag increases which indicated that the character of the boundary layer was approaching the fully turbulent condition. The pitching moments and lift coefficients were unaffected by variations in either grit size or Reynolds number.

## INTRODUCTION

During the development cycle of any aircraft, much wind-tunnel data are obtained on small-scale models in order to define the aerodynamic characteristics and performance qualities of the configuration. In order that the wind-tunnel data may be extrapolated to represent the full-scale aircraft, careful attention must be given during the tests to flow conditions in the model boundary layer. In most wind-tunnel investigations of this type, a boundary-layer trip is used to induce artificially a fully turbulent boundary layer on the model. The most effective methods commonly used to trip the boundary layer of wind-tunnel models consists of applying strips of either wire or distributed three-dimensional roughness particles near the leading edges of the various model components. (See refs. 1 to 3.) The wind-tunnel data can then be extrapolated by the turbulent-skin-friction formula since the flight Reynolds numbers for a full-scale airplane are usually of sufficient magnitude that turbulent flow naturally exists in the boundary layer over most of the aircraft. However, it is only when the trip successfully produces a fully turbulent boundary layer on the model that the wind-tunnel data can be extrapolated with confidence to full-scale conditions.

Reference 4 presents a simplified method for determining the critical height of distributed roughness particles which initiate the formation of turbulent spots at the roughness and coalesce into a continuously turbulent flow somewhat downstream of the roughness. However, an increase in roughness Reynolds number above the critical value is required to move the fully developed turbulent boundary layer to the roughness particles. References 5 and 6 present the effects of a wire trip on the boundary-layer transition and aerodynamic characteristics of several wing-body combinations at transonic speeds.

The purpose of this report is to present the results of an investigation to determine the effects of three-dimensional roughness trips on the boundary-layer transition and longitudinal aerodynamic characteristics of a wing-body-tail configuration at a Mach number of 1.61.

## SYMBOLS

All the data presented herein are referred to the stability-axis system, with the moment center located at 54.3 percent of the body length.

$C_D$	drag coefficient, $\frac{\text{Drag}}{qS}$
$\Delta C_D$	drag increment due to lift, $C_D - C_{D,o}$
$C_{D,f}$	skin-friction drag coefficient
$C_{D,o}$	zero-lift drag coefficient

$C_L$	lift coefficient, $\frac{\text{Lift}}{qS}$
$C_m$	pitching-moment coefficient, $\frac{\text{Pitching moment}}{qS\bar{c}}$
$\bar{c}$	reference chord, 1.002 ft
$L/D$	lift-drag ratio
$q$	free-stream dynamic pressure, lb/sq ft
$R$	free-stream Reynolds number
$S$	reference area, 1.092 sq ft
$\alpha$	angle of attack, deg

#### MODEL AND APPARATUS

A sketch of the model with dimensions is given in figure 1. The body was typical of a transport type of fuselage with an overall length of 39.32 inches and a maximum cross-sectional area of 5.625 square inches.

The wing was trapezoidal in planform and had a leading-edge sweep angle of  $62.1^\circ$  with an aspect ratio of 1.08 and a taper ratio of 0.255. The wing airfoil section was an NACA 0004.08-63 in the streamwise direction with a modification near the leading edge. The modification produced an essentially wedge-shaped section for the first 14 percent of the airfoil.

The horizontal tail had a leading-edge sweep angle of  $45^\circ$  and a negative dihedral angle of  $19^\circ$ . The airfoil was a 4.5-percent-thick biconvex section. The vertical tail had a leading-edge sweep angle of  $52^\circ$  and an NACA 0005-64 airfoil section.

The model was mounted in the Langley 4- by 4-foot supersonic pressure tunnel on a remotely controlled sting, and the forces and moments were measured by a six-component internal strain-gage balance.

#### TESTS AND CORRECTIONS

The tests were made at a Mach number of 1.61 and throughout a range of stagnation pressures which resulted in free-stream Reynolds numbers per foot from about 0.6 million to 8.0 million. The stagnation temperature was  $110^\circ\text{F}$  and the dewpoint was maintained sufficiently low to prevent any significant condensation effects in the test section.

Force and moment data were recorded throughout the range of test Reynolds numbers, with the model angle of attack adjusted to produce zero lift. Tests were made without boundary-layer trips and with trips of different roughness heights. At three test Reynolds numbers, force and moment data were recorded throughout an angle-of-attack range from about  $-1^{\circ}$  to  $12^{\circ}$  with several roughness sizes and without the trip.

The distributed three-dimensional roughness trips consisted of carborundum grit of various sizes, thinly spread in  $1/8$ -inch-wide strips. These strips were placed  $1/2$  inch back in the streamwise direction from the leading edges of the wing and body and  $1/4$  inch back on the horizontal and vertical tails. The roughness-particle sizes used in the investigation are shown in the following table:

Roughness grit number	Approximate mean height, in.
60	0.0117
80	.0083
120	.0049

The body base pressures were measured and the drag data were adjusted to correspond to a base pressure equal to free-stream static pressure. The angles of attack were corrected for the deflections of the balance and sting support system under load.

## PRESENTATION OF RESULTS

The results of the investigation are presented in the following figures:

	Figure
Effects of grit size on variation of zero-lift drag coefficient with Reynolds number . . . . .	2
Effects of grit size on longitudinal aerodynamic characteristics of model at a Reynolds number per foot of $2.80 \times 10^6$ . . . . .	3
Effects of Reynolds number on longitudinal aerodynamic characteristics of model with No. 120 grit . . . . .	4
Effects of Reynolds number on longitudinal aerodynamic characteristics of model without grit . . . . .	5
Effects of grit size on drag increment due to lift. $R = 2.80 \times 10^6$ per foot . . . . .	6

Effects of Reynolds number on drag increment due to lift of model with No. 120 grit . . . . .	7
Effects of Reynolds number on drag increment due to lift of model without grit . . . . .	8

## DISCUSSION

Figure 2 shows the effects of distributed roughness grit size on the variation of zero-lift drag coefficient with Reynolds number. Also shown on the figure are theoretical estimates of the drag levels for a fully laminar and a fully turbulent boundary layer. The variation in turbulent-skin-friction drag was estimated by means of the Kármán-Schoenherr incompressible formula and the Sommer and Short T' method (ref. 7). The variation in laminar-skin-friction drag was estimated by the Chapman-Rubesin formula (ref. 8). For both the laminar and the turbulent conditions, the wave-drag coefficient was assumed to be 0.0092.

For each of the tests for which transition strips were applied to the model, the drag approached the theoretical turbulent curve with increasing Reynolds number and then decreased along the curve with further increases in the free-stream Reynolds number. At the highest Reynolds numbers per foot ( $R > 6.0 \times 10^6$ ), the drag levels appear to exceed the theoretical turbulent level. This additional drag may be due to the roughness particles since at these Reynolds numbers the roughness-particle height is larger than the boundary-layer thickness. As would be expected, the data indicate that the larger roughness particles (smaller grit number) approach the theoretical turbulent curve and thereby indicate a fully turbulent boundary layer at a lower free-stream Reynolds number than the smaller roughness particles. There was, however, little difference between the drag variations of the model with No. 80 grit and with No. 120 grit. When transition strips were not applied to the model, the zero-lift drag coefficient remained relatively constant throughout the range of Reynolds numbers that were investigated and never indicated a fully turbulent boundary layer. Within the range of unit Reynolds numbers, from a point where the data begin to be parallel to the theoretical turbulent curve and the boundary-layer flow becomes fully turbulent to a point where the data begin to exceed the theoretical curve, the drag data fall within a band which has a maximum width of about 0.0005. Since the width of this band is about equal to the estimated accuracy of the drag data based on repeatability and static calibrations of the balance, it can be seen that within this range of unit Reynolds numbers the drag increments due to the various sizes of roughness particles are small and within the accuracy of the drag data.

As can be seen in figures 3 to 5, the pitching moments and lift coefficients were unaffected by variations in either grit size or Reynolds number. However, as would be expected, the drag coefficients and lift-drag ratios were significantly affected by flow conditions in the model boundary layer. At a unit Reynolds number per foot of  $2.80 \times 10^6$  the model boundary-layer flow is essentially turbulent for each of the grit sizes (fig. 2). However, for the models without the grit applied, a rather large increase in unit Reynolds number is

required to produce fully turbulent flow at zero lift. When the drag levels for the model with and without grit are compared (fig. 3), it can be seen that the increment decreases as small values of lift are attained and remains constant as the lift is further increased. This fact suggests that the small amount of lift produced an increase in the amount of turbulent flow in the model boundary layer.

The aerodynamic characteristics of the model with transition strips of No. 120 grit are compared at three values of free-stream unit Reynolds number in figure 4. At the highest unit Reynolds number per foot of  $2.80 \times 10^6$ , the flow at zero lift appears to be fully turbulent (fig. 2), whereas at the lower Reynolds numbers relatively large amounts of laminar flow are indicated. As the lift coefficient is increased to a value of about 0.15, the relatively large increments in the model drag level disappear, indicating that the model boundary layer is approaching the fully turbulent condition. (See fig. 4.) In the region of maximum lift-drag ratio, the  $C_D$  and  $L/D$  values were essentially unaltered by changes in the test Reynolds number.

A comparison of the aerodynamic characteristics of the model without transition strips at two values of free-stream unit Reynolds number (fig. 5) indicates little difference in the lift-drag ratio and drag-coefficient levels, even though relatively large amounts of laminar flow were indicated in both cases at zero lift (fig. 2).

Figures 6 to 8 show the effects of grit size and Reynolds number on the drag increment due to lift as a function of the lift coefficient squared. Also shown for reference as a dashed line is the  $\Delta C_D$  for a symmetrical drag polar having a drag-due-to-lift factor  $\Delta C_D/C_L^2$  of 0.435. The drag polar for this configuration is symmetrical about  $C_L = 0$ , and for the fully turbulent cases (grit on and  $R = 2.80 \times 10^6$  per foot) the variation of drag with  $C_L^2$  is essentially linear. However, it can be seen in each of the figures 6 to 8 that when significant amounts of laminar flow exist at zero lift, the drag due to lift departs from a linear variation at the low lift coefficients and indicates a higher drag due to lift at the higher lift coefficients. This effect is due to the increase in skin-friction drag as the model boundary layer approaches the fully turbulent condition.

#### CONCLUDING REMARKS

A wind-tunnel investigation has been conducted to determine the effects of three-dimensional roughness trips on the boundary-layer transition and the longitudinal aerodynamic characteristics of a wing-body-tail configuration at a Mach number of 1.61. The data indicate that the larger roughness particles produce a fully turbulent boundary layer at a lower free-stream Reynolds number than the smaller roughness particles. At the highest Reynolds numbers per foot (greater than about  $6.0 \times 10^6$ ), the drag levels appear to exceed the theoretical turbulent level. This additional drag may be due to the roughness particles since at these Reynolds numbers the roughness-particle height is larger than the



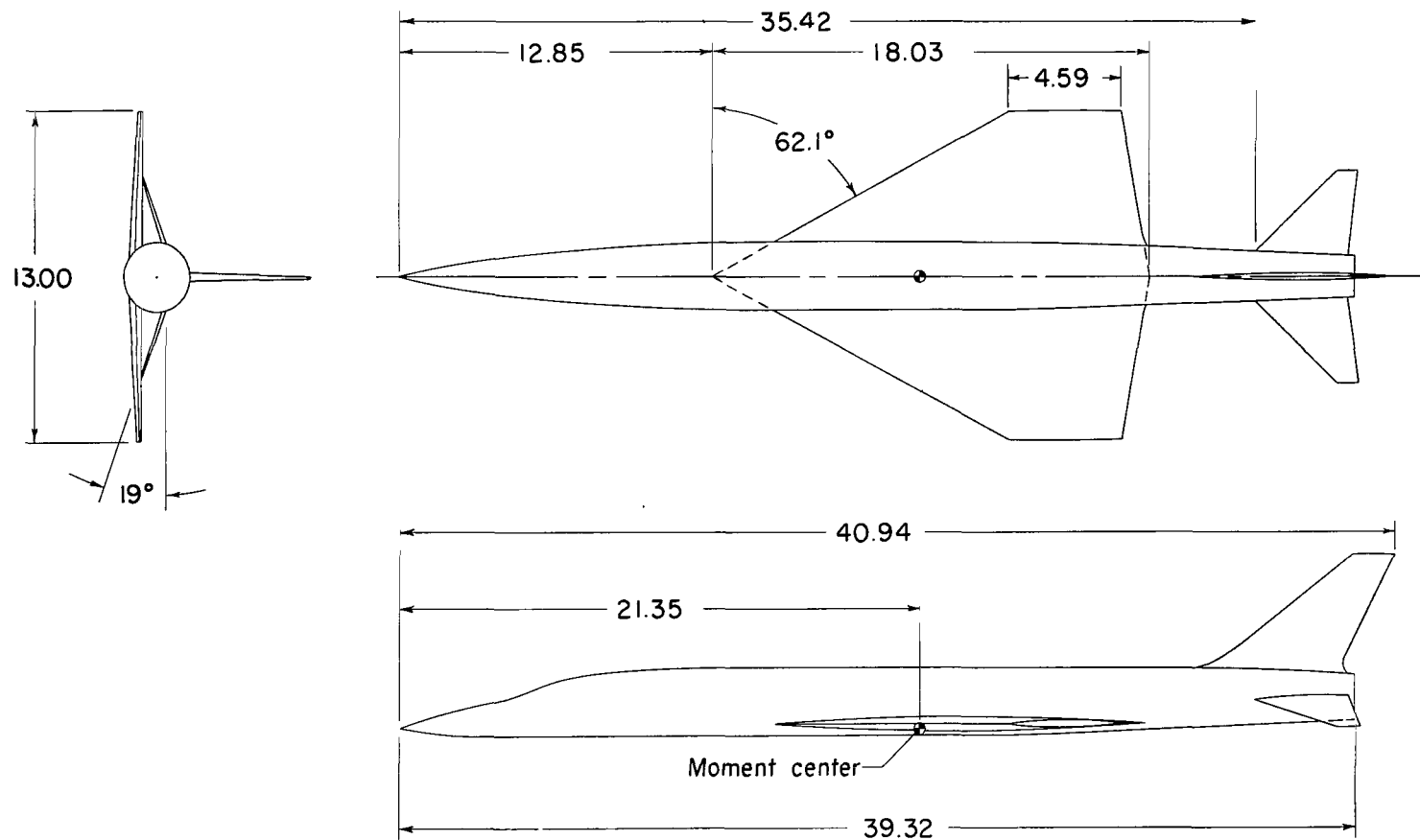
boundary-layer thickness. Within the range of Reynolds numbers for which the variations in zero-lift drag coefficient indicate fully turbulent flow in the model boundary layer, the drag increments due to the various sizes of roughness particles are small and within the accuracy of the drag data.

When the boundary layer was not fully turbulent at zero lift, small increases in the lift coefficient produced drag increases which indicated that the boundary layer was approaching the fully turbulent condition. The pitching moments and lift coefficients were unaffected by variations in either grit size or Reynolds number.

Langley Research Center,  
National Aeronautics and Space Administration,  
Langley Station, Hampton, Va., March 12, 1964.

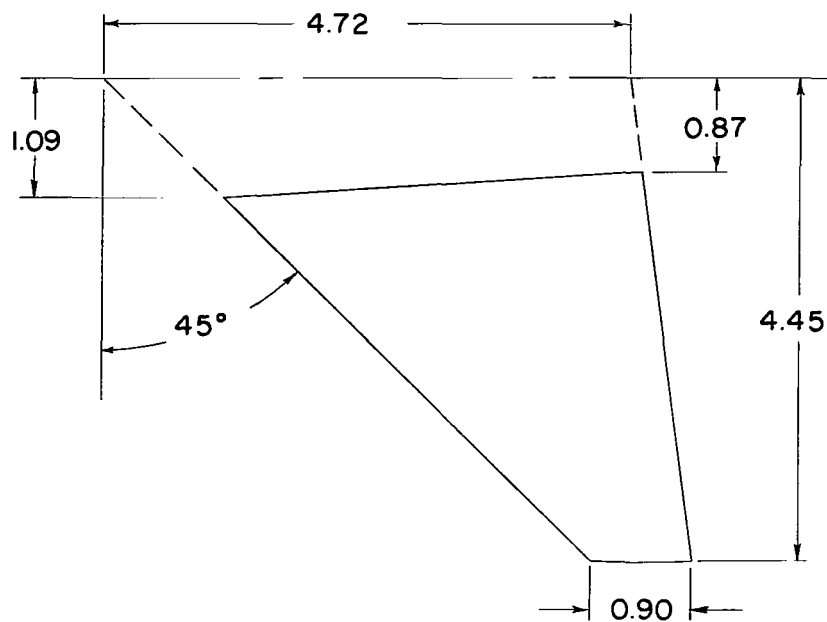
## REFERENCES

1. Braslow, Albert L., Knox, Eugene C., and Horton, Elmer A.: Effect of Distributed Three-Dimensional Roughness and Surface Cooling on Boundary-Layer Transition and Lateral Spread of Turbulence at Supersonic Speeds. NASA TN D-53, 1959. (Supersedes NACA RM L58A17.)
2. Czarnecki, K. R., and Sevier, John R., Jr.: Investigation of Effects of Roughness, Surface Cooling, and Shock Impingement on Boundary-Layer Transition on a Two-Dimensional Wing. NASA TN D-417, 1960.
3. Jackson, Mary W., and Czarnecki, K. R.: Investigation by Schlieren Technique of Methods of Fixing Fully Turbulent Flow on Models at Supersonic Speeds. NASA TN D-242, 1960.
4. Braslow, Albert L., and Knox, Eugene C.: Simplified Method for Determination of Critical Height of Distributed Roughness Particles for Boundary-Layer Transition at Mach Numbers From 0 to 5. NACA TN 4363, 1958.
5. Hunton, Lynn W.: Effects of Fixing Transition on the Transonic Aerodynamic Characteristics of a Wing-Body Configuration at Reynolds Numbers From 2.4 to 12 Million. NACA TN 4279, 1958.
6. Stivers, Louis S., Jr.: Effects of Fixing Boundary-Layer Transition for a Swept- and a Triangular-Wing and Body Combination at Mach Numbers From 0.60 to 1.40. NASA TN D-312, 1960.
7. Sommer, Simon C., and Short, Barbara J.: Free-Flight Measurements of Turbulent-Boundary-Layer Skin Friction in the Presence of Severe Aerodynamic Heating at Mach Numbers From 2.8 to 7.0. NACA TN 3391, 1955.
8. Chapman, Dean R., and Rubesin, Morris W.: Temperature and Velocity Profiles in the Compressible Laminar Boundary Layer With Arbitrary Distribution of Surface Temperature. Jour. Aero. Sci., vol. 16, no. 9, Sept. 1949, pp. 547-565.

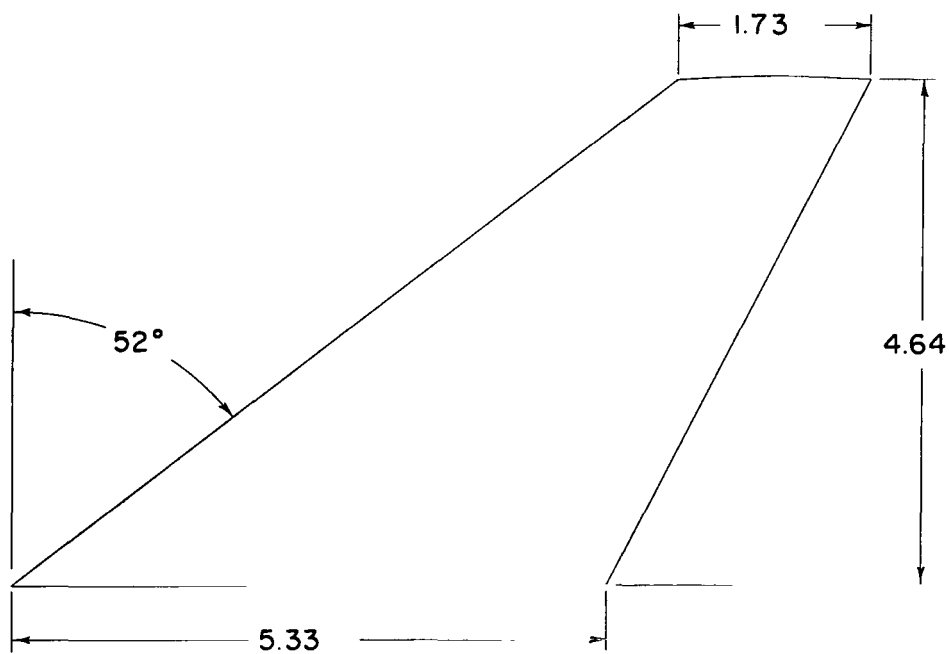


(a) Complete model.

Figure 1.- Description of model. All dimensions are in inches unless otherwise specified.



(b) Horizontal tail.



(c) Vertical tail.

Figure 1.- Concluded.

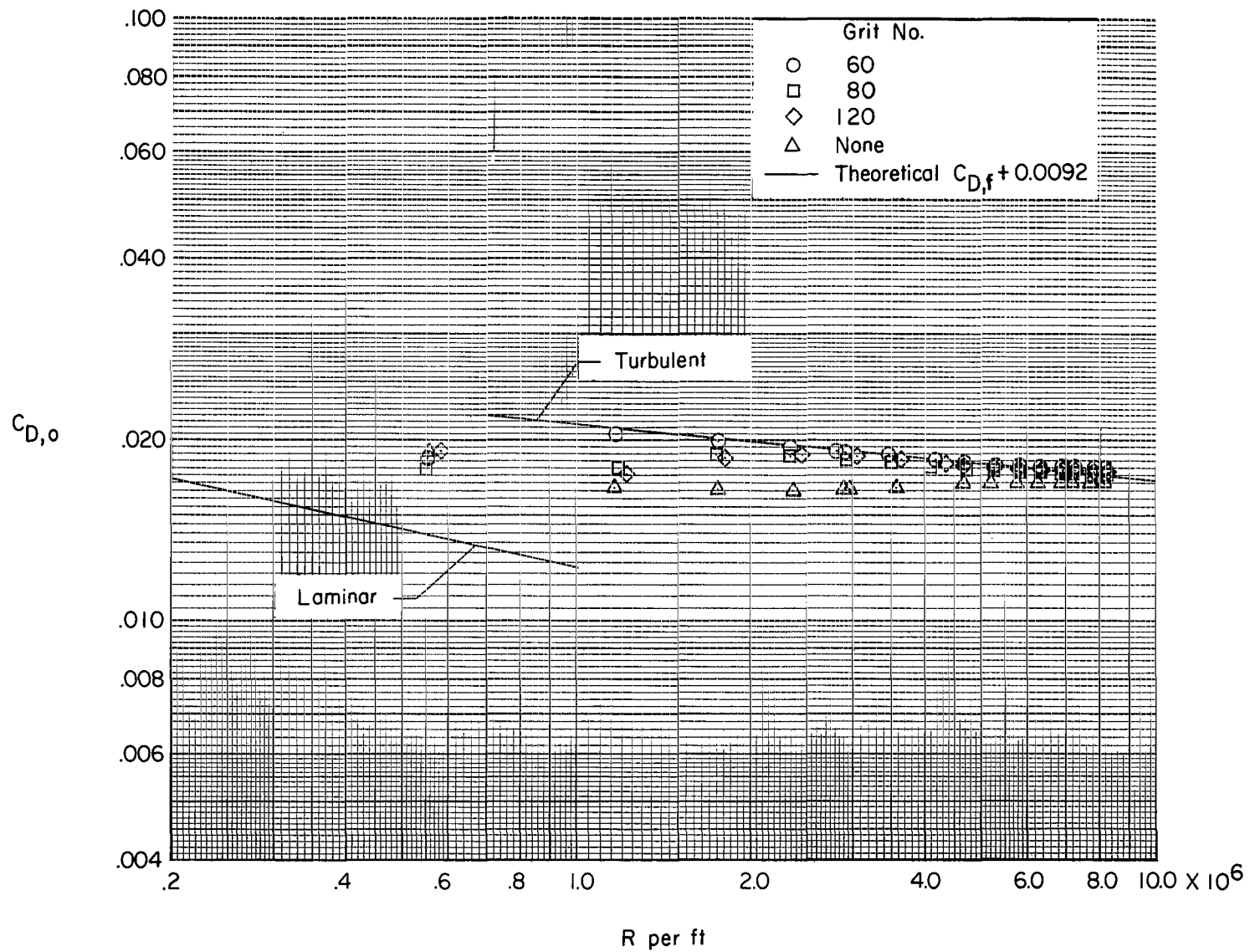


Figure 2.- Effects of grit size on variation of zero-lift drag coefficient with Reynolds number.

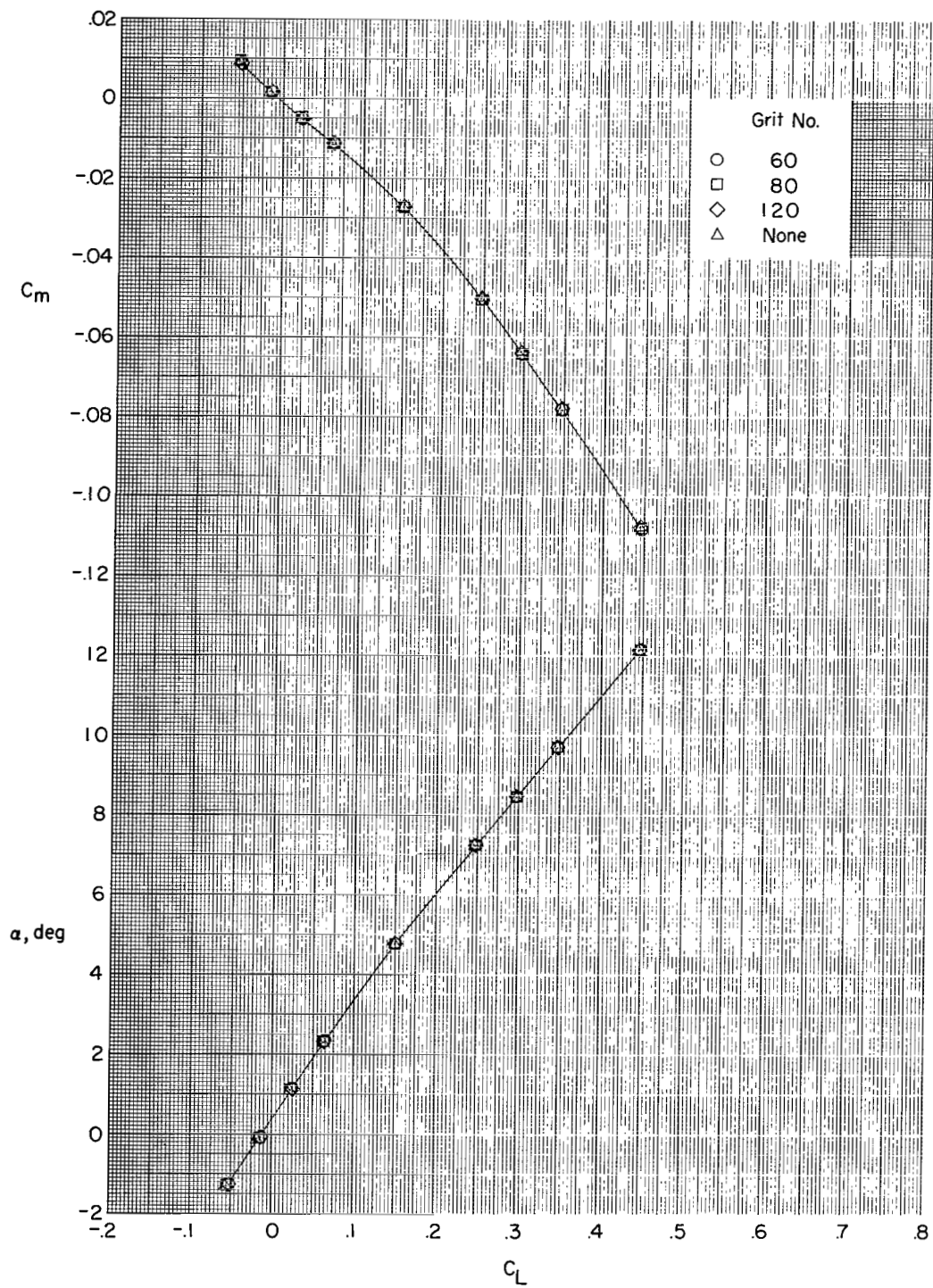


Figure 3.- Effects of grit size on longitudinal aerodynamic characteristics of model at a Reynolds number per foot of  $2.80 \times 10^6$ .

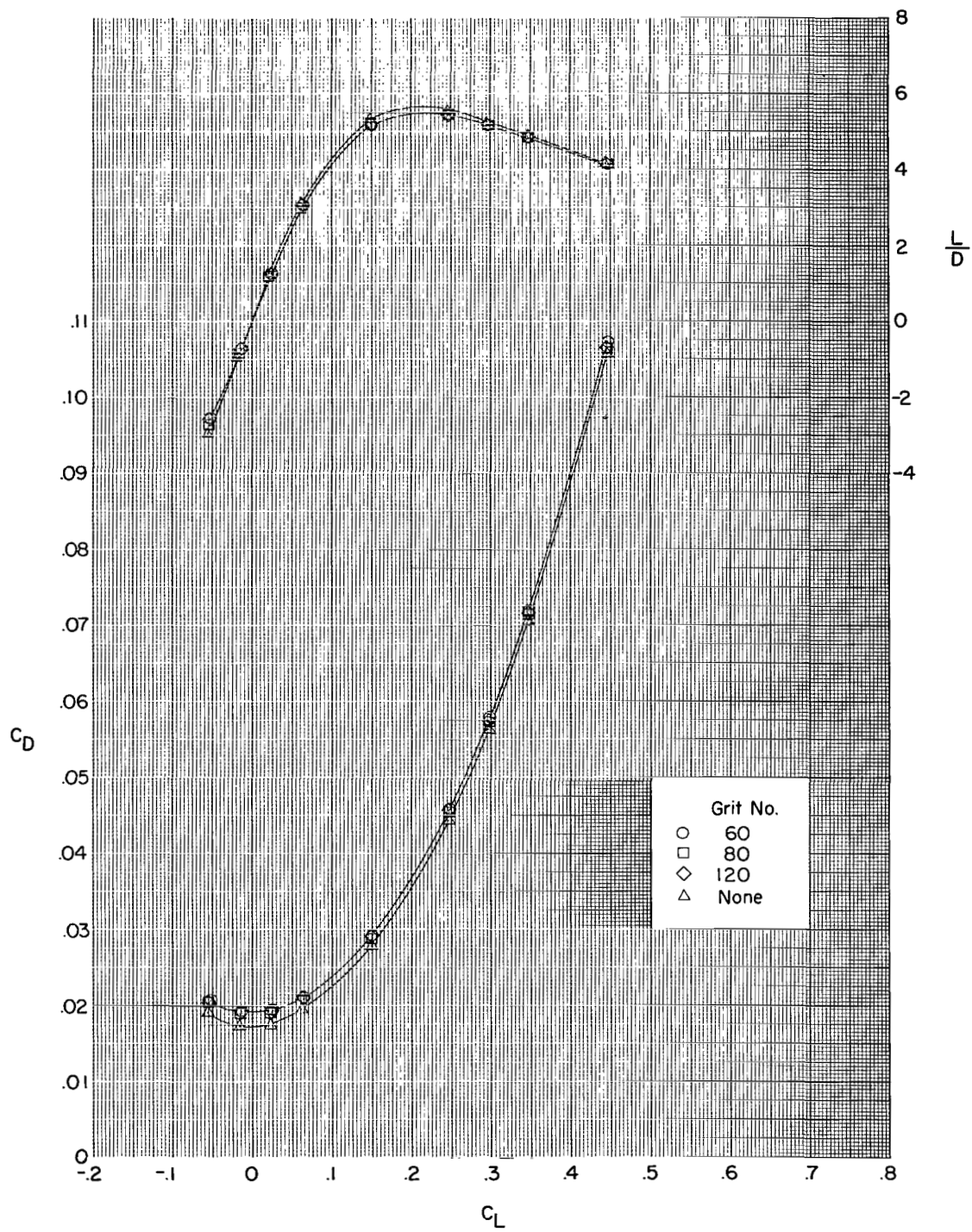


Figure 3.- Concluded.

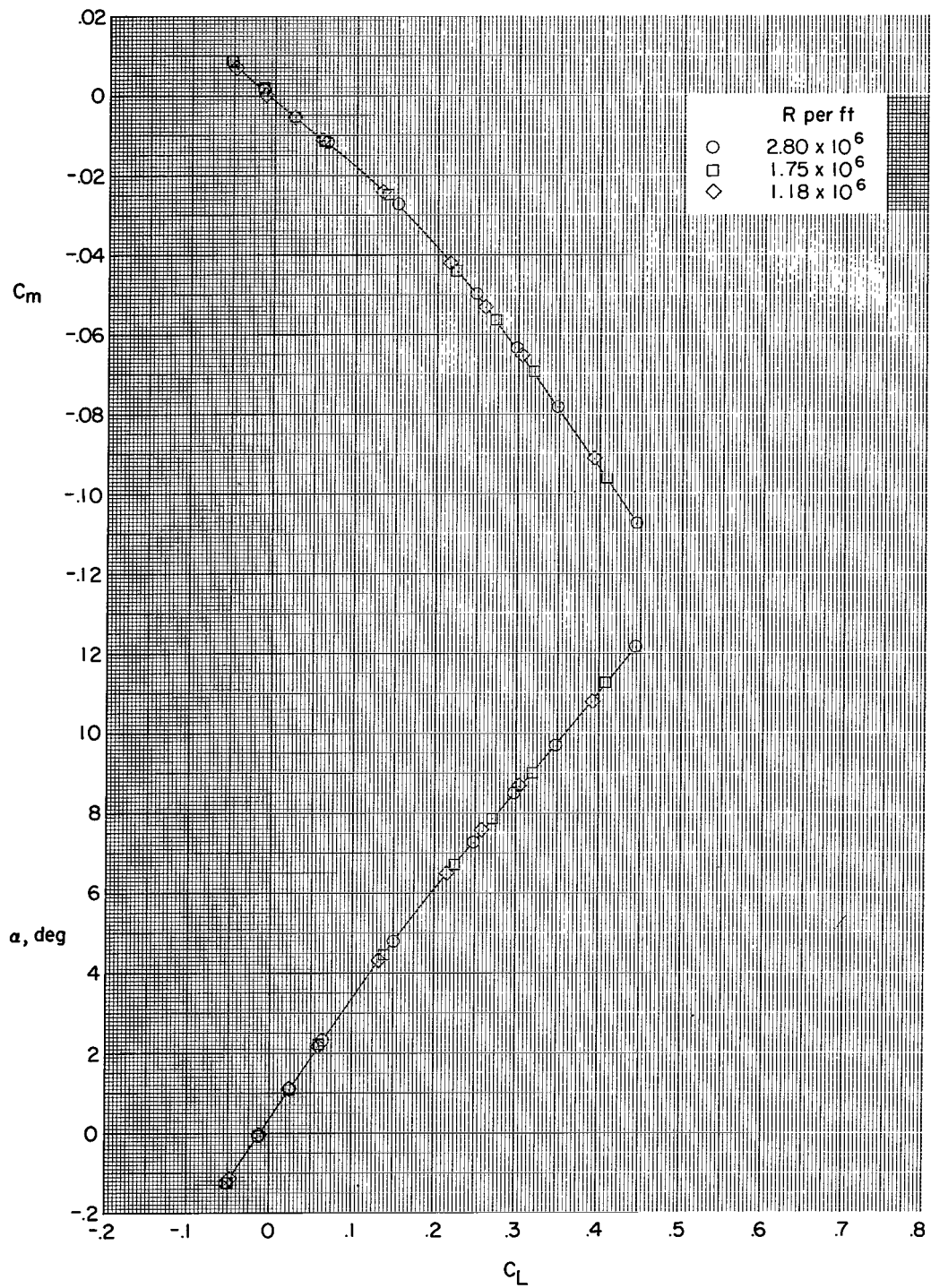


Figure 4.- Effects of Reynolds number on longitudinal aerodynamic characteristics of model with No. 120 grit.



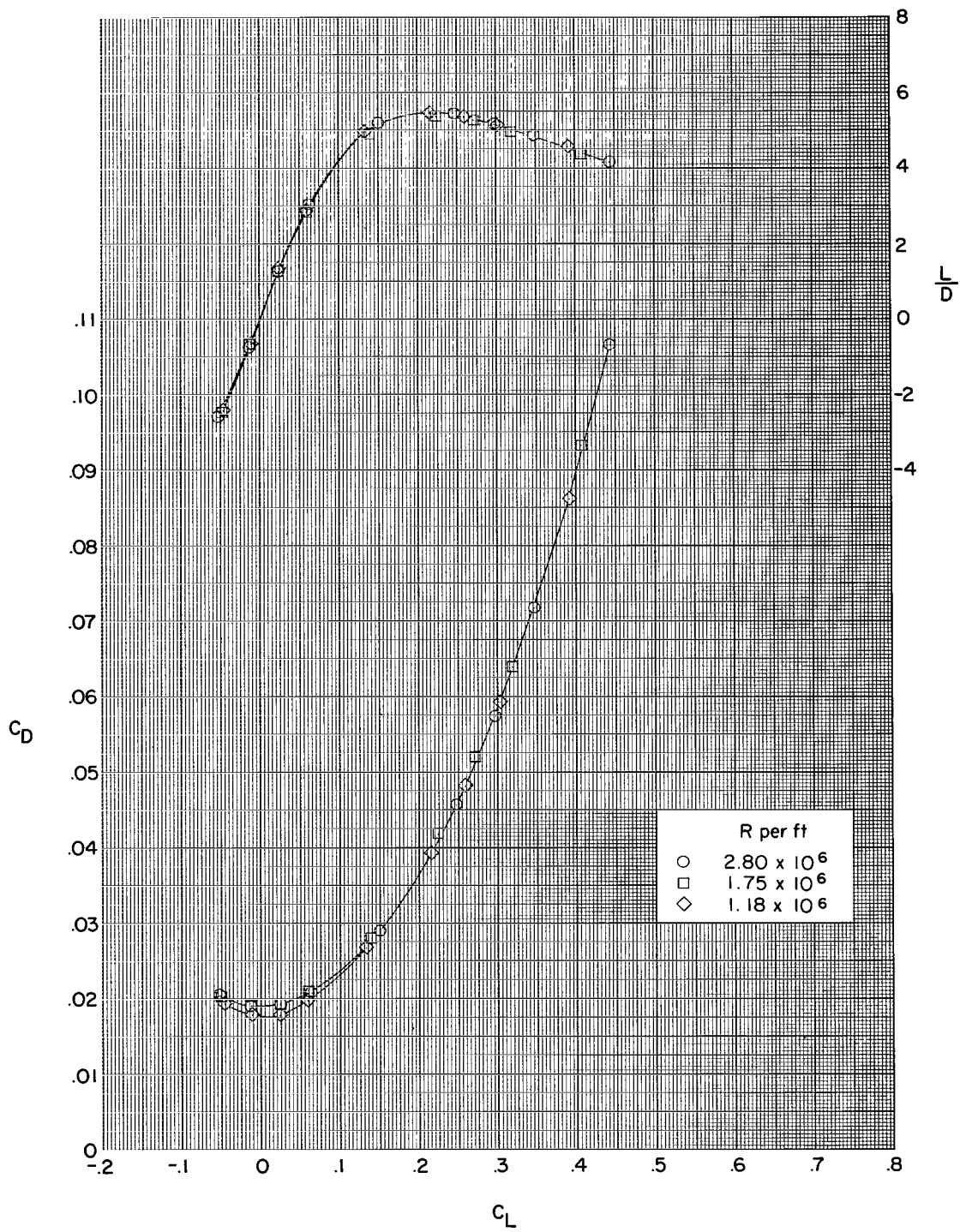


Figure 4.- Concluded.

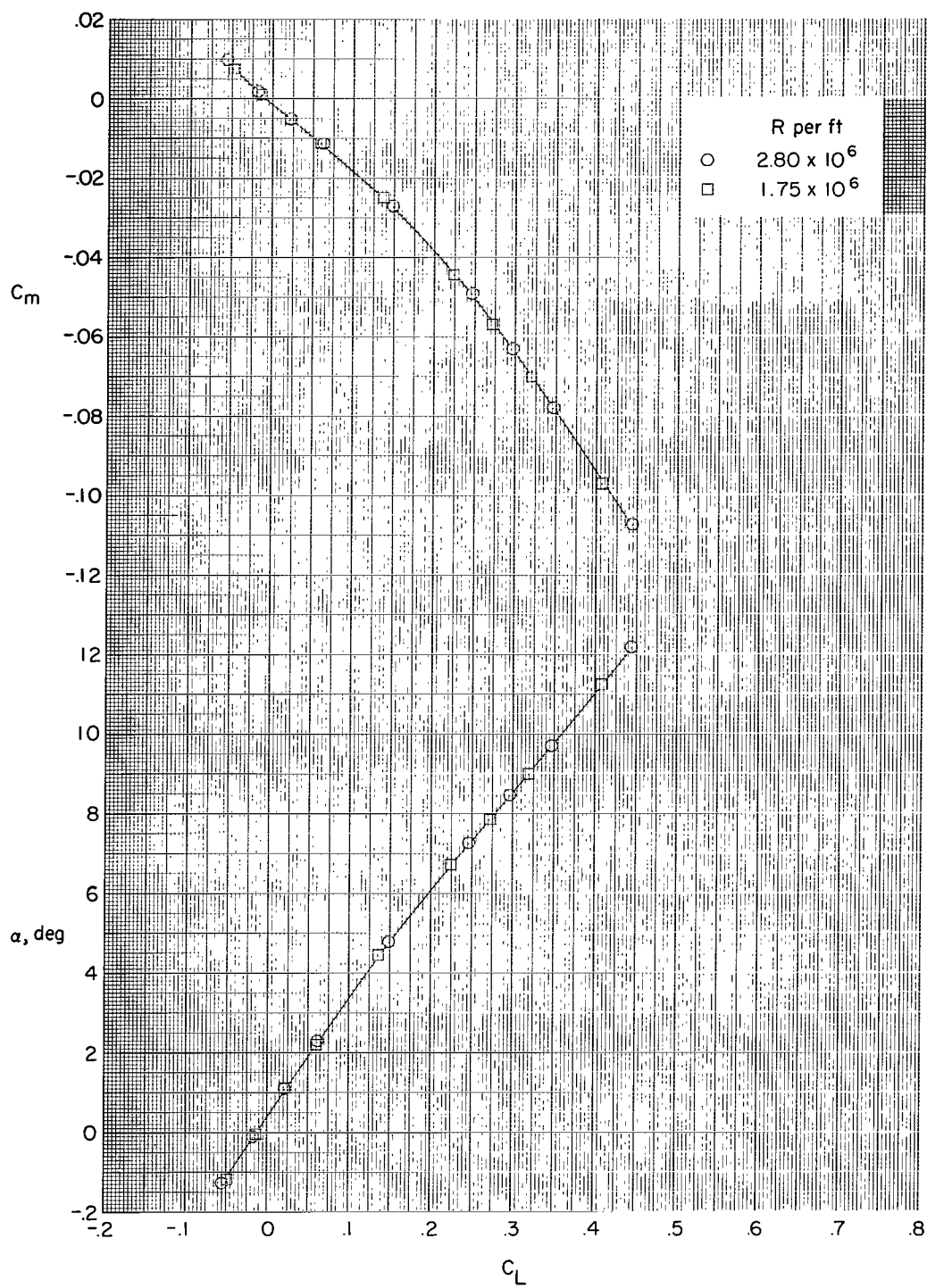


Figure 5.- Effects of Reynolds number on longitudinal aerodynamic characteristics of model without grit.

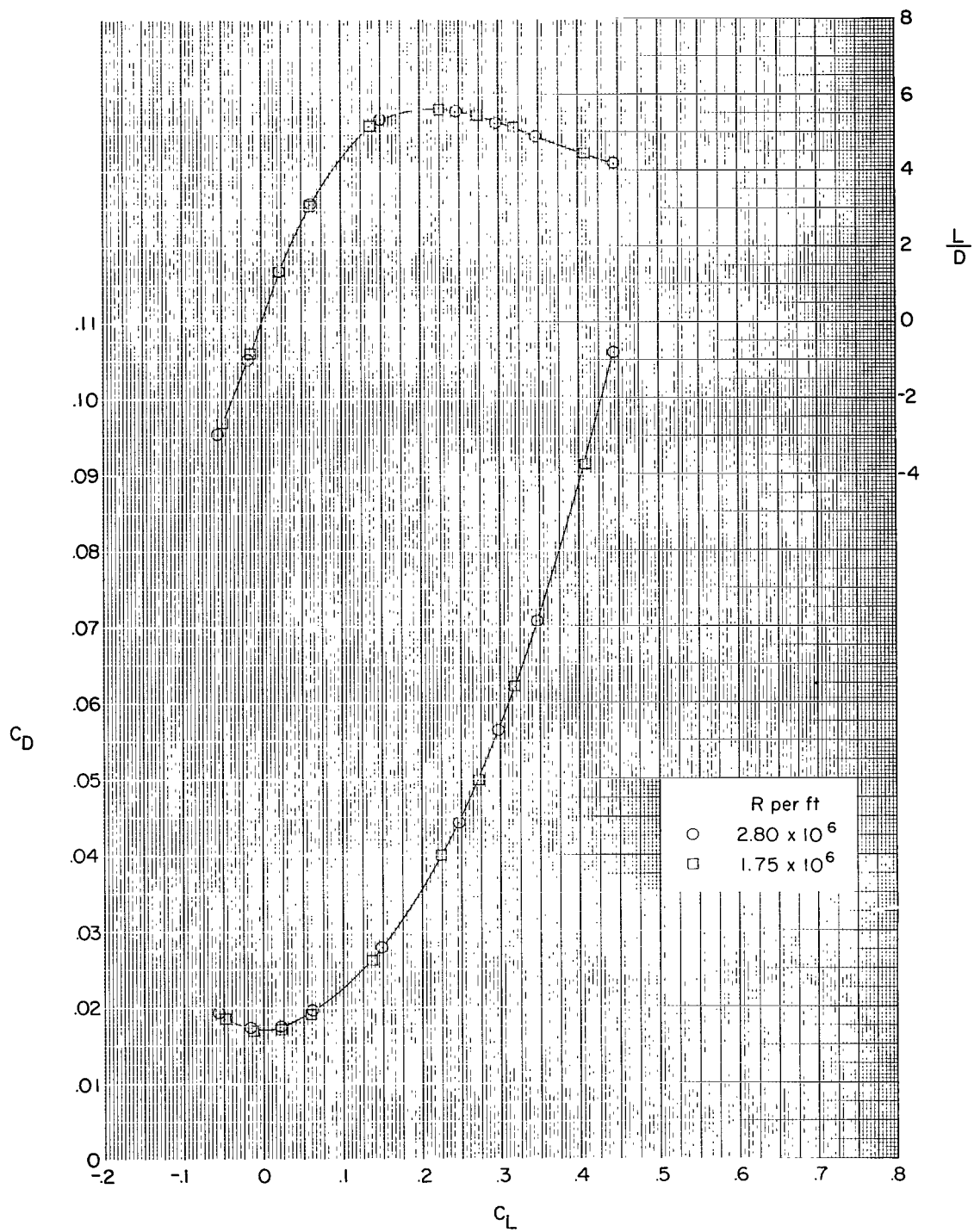


Figure 5.- Concluded.

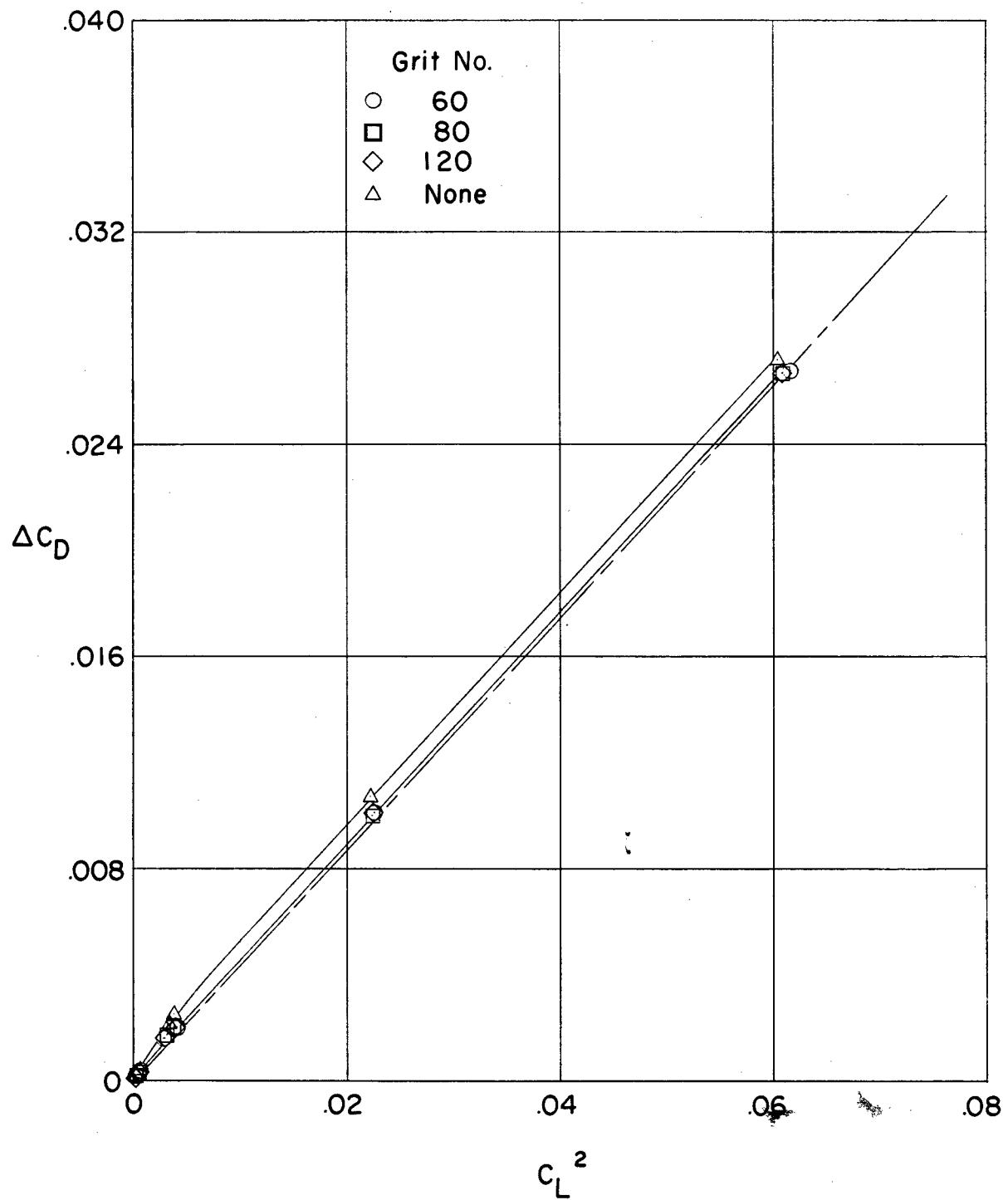


Figure 6.- Effects of grit size on drag increment due to lift.  $R = 2.80 \times 10^6$  per foot.  
(Dashed line indicates  $\Delta C_D$  for a symmetrical drag polar with  $\Delta C_D/C_L^2 = 0.435$ .)

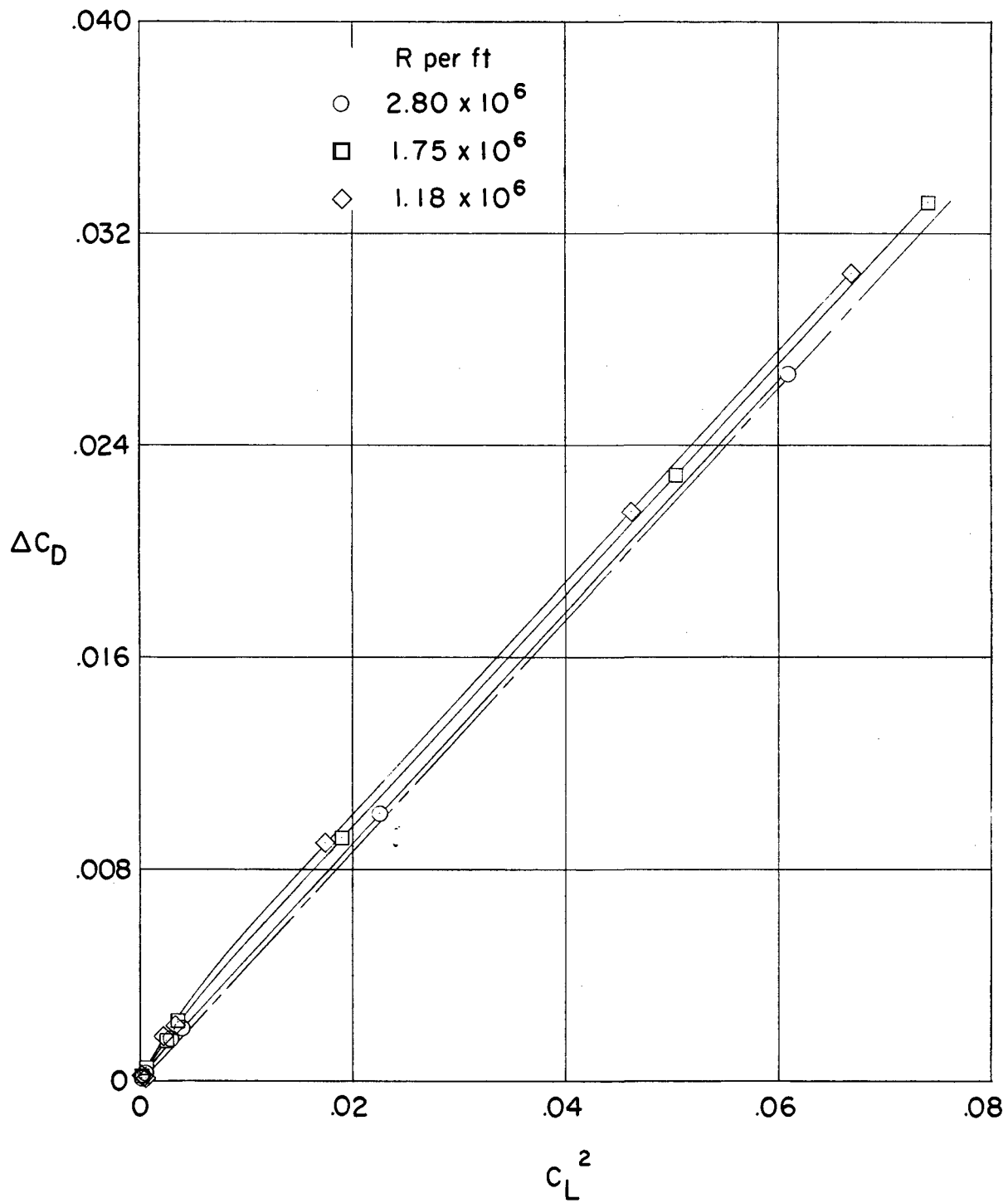


Figure 7.- Effects of Reynolds number on drag increment due to lift of model with No. 120 grit.  
(Dashed line indicates  $\Delta C_D$  for a symmetrical drag polar with  $\Delta C_D/C_L^2 = 0.435$ .)

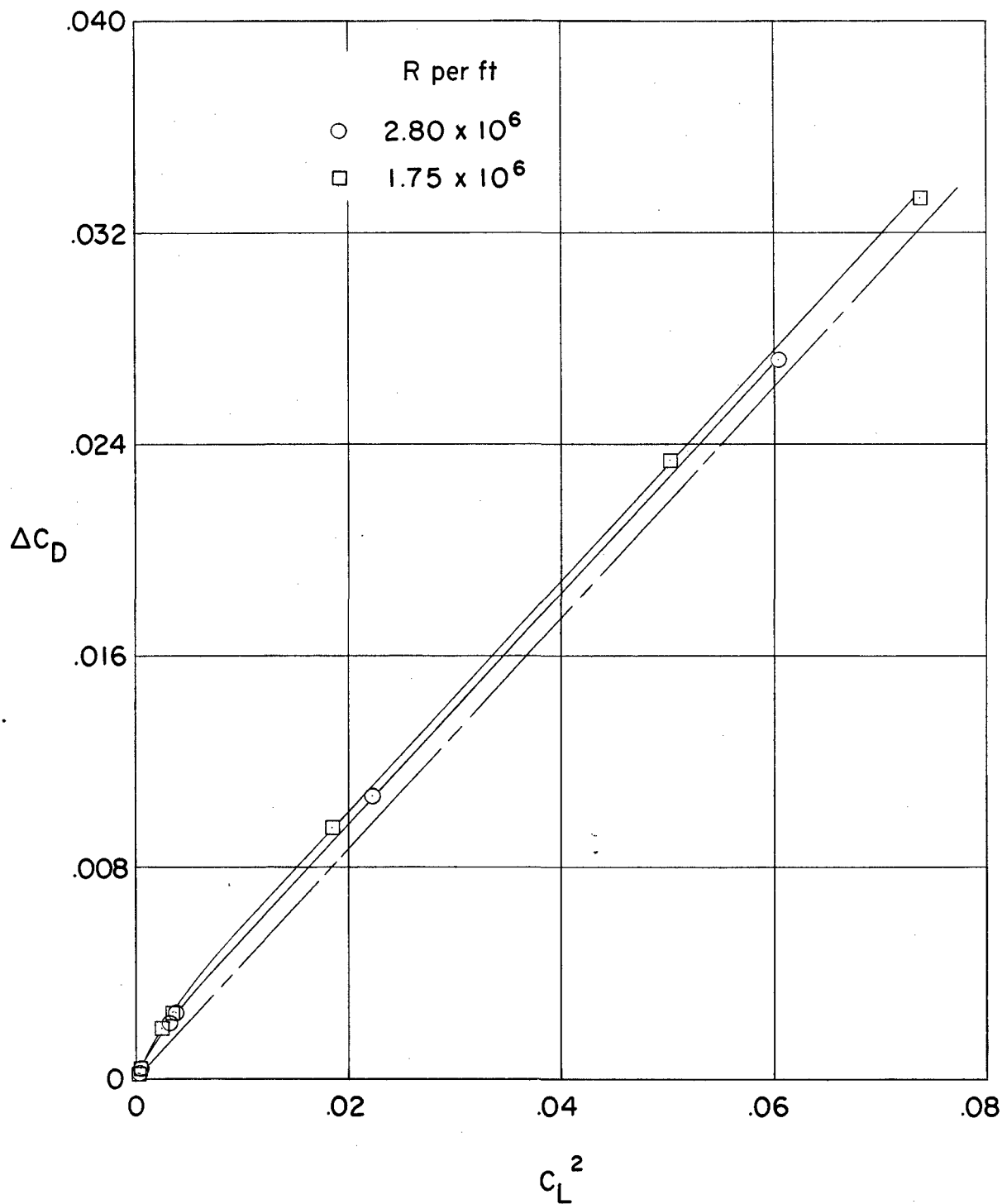


Figure 8.- Effects of Reynolds number on drag increment due to lift of model without grit.  
 (Dashed line indicates  $\Delta C_D$  for a symmetrical drag polar with  $\Delta C_D / C_L^2 = 0.435$ .)

217/85  
6

*"The aeronautical and space activities of the United States shall be conducted so as to contribute . . . to the expansion of human knowledge of phenomena in the atmosphere and space. The Administration shall provide for the widest practicable and appropriate dissemination of information concerning its activities and the results thereof."*

—NATIONAL AERONAUTICS AND SPACE ACT OF 1958

## NASA SCIENTIFIC AND TECHNICAL PUBLICATIONS

**TECHNICAL REPORTS:** Scientific and technical information considered important, complete, and a lasting contribution to existing knowledge.

**TECHNICAL NOTES:** Information less broad in scope but nevertheless of importance as a contribution to existing knowledge.

**TECHNICAL MEMORANDUMS:** Information receiving limited distribution because of preliminary data, security classification, or other reasons.

**CONTRACTOR REPORTS:** Technical information generated in connection with a NASA contract or grant and released under NASA auspices.

**TECHNICAL TRANSLATIONS:** Information published in a foreign language considered to merit NASA distribution in English.

**TECHNICAL REPRINTS:** Information derived from NASA activities and initially published in the form of journal articles.

**SPECIAL PUBLICATIONS:** Information derived from or of value to NASA activities but not necessarily reporting the results of individual NASA-programmed scientific efforts. Publications include conference proceedings, monographs, data compilations, handbooks, sourcebooks, and special bibliographies.

*Details on the availability of these publications may be obtained from:*

SCIENTIFIC AND TECHNICAL INFORMATION DIVISION  
NATIONAL AERONAUTICS AND SPACE ADMINISTRATION  
Washington, D.C. 20546